# Electrodeposition of Three-Dimensional Titania Photonic Crystals from Holographically Patterned Microporous Polymer Templates

Yongan Xu,[†] Xuelian Zhu,[†] Yaping Dan,[‡] Jun Hyuk Moon,[†] Vincent W. Chen,[§] Alan T. Johnson,[||] Joseph W. Perry,[§] and Shu Yang*,[†]

*Department of Materials Science & Engineering, University of Pennsylvania, Philadelphia, Pennsylvania 19104, Department of Electrical and Systems Engineering, University of Pennsylvania, 200 South 33rd Street, Philadelphia, Pennsylvania 19104, School of Chemistry and Biochemistry and Center for Organic Photonics and Electronics, Georgia Institute of Technology, Atlanta, Georgia 30332-0400, and Department of Physics and Astronomy, University of Pennsylvania, 209 South 33rd Street, Philadelphia, Pennsylvania 19104*

*Received September 3, 2007. Revised Manuscript Received December 9, 2007*

To fabricate a photonic crystal with large and complete photonic bandgap, it often requires backfilling of high index inorganic materials into a 3D polymer template. However, the pore network may become disconnected before the template is completely filled in a conformal coating process, which, therefore, limits the achievable maximum bandgap in the 3D photonic crystals. Here, we demonstrate nearly complete filling of the holographically patterned, diamond-like polymer templates with titania sol−gel through the electrodeposition method. The deposition proceeded in two stages: a thin titania seed layer (∼55 nm thick) was conformally coated on the surface of the polymer template at the early stage of electrodeposition, after which the deposition occurred preferentially from the template bottom layer at a rate of ∼0.4 $\mu$m/min. After preannealing and a slow ramping rate to 500 °C to remove the polymer template, an inverse 3D anatase titania crystal was obtained without pattern collapse. The measurement of film reflectivity in the [111] direction before and after the deposition in comparison to the calculated photonic bandgap properties suggested that (1) the template was nearly completely filled by the electrodeposition process and (2) the photonic structure was well-preserved after the removal of the template.

## Introduction

Photonic crystals with periodic modulation in refractive index or dielectric constant are of interest for numerous applications in integrated optical circuits, such as enhancing the performance of semiconductor lasers, waveguides, and all on chip optical transistors.[1] Interference of the light waves scattered from the three-dimensional (3D) photonic crystal could prohibit light from any direction in a range of frequencies, leading to complete photonic bandgaps (PBGs).[2,3] The bandwidth and the frequency of the PBG are determined by the refractive index contrast, the structure symmetry, and the volume fraction of high-index materials.

Major progress has been made in developing different methods of fabricating 3D microstructures.[4] However, the low refractive index of the patterned film ($n < 1.7$) has become the bottleneck that limits the realization of complete PBGs in the fabricated 3D crystals. The minimum required refractive index contrast to open a bandgap is 1.8 for a diamond D structure.[5] Therefore, many begin to investigate the backfilling of high index materials, including titania ($n = 2.2-3.0$),[6] selenium ($n = 2.5$),[7] cadmium−selenium ($n = 2.5-2.75$),[8] amorphous silicon ($n = 3.5$),[9–14] and germanium ($n = 4.0$),[15] using the fabricated 3D structures as templates. These inorganic materials can be deposited through either a dry process, including chemical vapor deposition (CVD),[9−14] atomic layer deposition (ALD),[16,17] and melting,[7] or wet chemical methods, including liquid

* Corresponding author. Tel.: (215) 898-9645. Fax: (215) 573-2128. E-mail: shuyang@seas.upenn.edu.
[†] Department of Materials Science & Engineering, University of Pennsylvania.
[‡] Department of Electrical and Systems Engineering, University of Pennsylvania.
[§] Georgia Institute of Technology.
[||] Department of Physics and Astronomy, University of Pennsylvania.

(1) Joannopoulos, J. D.; Meade, R. D.; Winn, J. N. *Photonic Crystals*; Princeton University Press: Princeton, NJ, 1995.
(2) John, S. *Phys. Rev. Lett.* **1987**, *58*, 2486.
(3) Yablonovitch, E. *Phys. Rev. Lett.* **1987**, *58*, 2059.
(4) Moon, J. H.; Ford, J.; Yang, S. *Polym. Adv. Technol.* **2006**, *17*, 83.
(5) Maldovan, M.; Urbas, A. M.; Yufa, N.; Carter, W. C.; Thomas, E. L. *Phys. Rev. B* **2002**, 65.
(6) Wijnhoven, J.; Bechger, L.; Vos, W. L. *Chem. Mater.* **2001**, *13*, 4486.
(7) Braun, P. V.; Zehner, R. W.; White, C. A.; Weldon, M. K.; Kloc, C.; Patel, S. S.; Wiltzius, P. *Adv. Mater.* **2001**, *13*, 721.
(8) Braun, P.; Wiltzius, P. *Adv. Mater.* **2001**, *13*, 482.
(9) Vlasov, Y. A.; Bo, X.-Z.; Sturm, J. C.; Norris, D. J. *Nature* **2001**, *414*, 289.
(10) Miguez, H.; Tetreault, N.; Yang, S. M.; Kitaev, V.; Ozin, G. A. *Adv. Mater.* **2003**, *15*, 597.
(11) Tétreault, N.; Miguez, H.; Ozin, G. A. *Adv. Mater.* **2004**, *16*, 1471.
(12) Tétreault, N.; von Freymann, G.; Deubel, M.; Hermatschweiler, M.; Pérez-Willard, F.; John, S.; Wegener, M.; Ozin, G. A. *Adv. Mater.* **2006**, *18*, 457.
(13) Gratson, G. M.; Garcia-Santamaria, F.; Lousse, V.; Xu, M. J.; Fan, S. H.; Lewis, J. A.; Braun, P. V. *Adv. Mater.* **2006**, *18*, 461.
(14) Moon, J. H.; Yang, S.; Dong, W. T.; Perry, J. W.; Adibi, A.; Yang, S. M. *Opt. Express* **2006**, *14*, 6297.
(15) Miguez, H.; Meseguer, F.; Lopez, C.; Holgado, M.; Andreasen, G.; Mifsud, A.; Fornes, V. *Langmuir* **2000**, *16*, 4405.
(16) King, J. S.; Graugnard, E.; Roche, O. M.; Sharp, D. N.; Scrimgeour, J.; Denning, R. G.; Turberfield, A. J.; Summers, C. J. *Adv. Mater.* **2006**, *18*, 1561.
(17) Graugnard, E.; King, J. S.; Gaillot, D. P.; Summers, C. J. *Adv. Funct. Mater.* **2006**, *16*, 1187.

10.1021/cm702511k CCC: $40.75 
Published on Web 02/05/2008

phase sol−gel reaction, electrochemical reaction,[8] and precipitation.[18,19] Most templates studied for backfilling, however, are from closely packed colloidal crystals, which have narrow bandgaps.

Recently, triply periodic bicontinuous structures (e.g., simple cubic P, gyroid G, and diamond D), which can be patterned by holographic lithography, have received increasing interest because they possess wide, complete PBGs.[5,20,21] The study of the backfilling of holographically patterned polymer templates through sequential silica/silicon CVD[14] and ALD[16] processes, however, finds it challenging to completely fill the triply periodic bicontinuous templates. In the top-down infiltration processes, core−shell morphology is often revealed as the deposited materials grow conformally and continuously on the 3D template surface to fill the interstitial pores. Because the pore sizes are not uniform throughout the bicontinuous template, the surface of the pore network tends to pinch off (i.e., disconnects) at the narrowest pore channels before the interstitial voids are completely filled,[14,22] resulting in loss of photonic bandgap properties.[22,23] In contrast, wet chemical methods have been demonstrated by Meldrum et al. to achieve maximal filling of inorganic materials,[19,24–26] including $CaCO_3$, $SrSO_4$, $PbSO_4$, $PbCO_3$, NaCl, Au, Ni, and Cu, in the macroporous simple cubic polymer templates (pore size of 10−15 $\mu$m), which were replicated from the sea urchin skeletal plates.

Of many wet chemical methods, electrodeposition is particularly suitable for growing functional materials into complex 3D geometries. It has been commonly used in the microelectronic industry, often referred to as an electroplating process, to fill the deep through-holes in electrical interconnects and printed circuit boards.[27] It possesses some unique characteristics, including (1) deposition occurring preferentially in the bottom of the structure,[27] (2) room temperature reaction from water-based electrolytes, and (3) the ability to fill small pores (diameter $\leq$ 20 nm).[28] Typically the electrodeposited materials grow from the the conductive substrate outward.

High-index inorganic materials, including CdSe,[29] CdS,[8] ZnO,[30] GaAs,[31] and $TiO_2$,[28] have been deposited in colloidal templates and nanoporous channels using potentiostatic[32] and galvanostatic[33] deposition methods. Specifically, Miao et al.[28] have grown $TiO_2$ nanowire arrays from anodic aluminum oxide (AAO) membranes through electrochemically induced sol−gel reaction. The pores are nearly completely filled from the bottom to the top with very high aspect ratios (diameter as small as 10 nm and length up to 10 $\mu$m). Using a procedure modified from Miao et al., we have shown some preliminary success to electrodeposit titania sol−gel in a holographically patterned, diamond-like polymer template.[22] It is yet to be studied, however, whether the titania sol−gel is selectively and completely filled within the 3D polymer template with variable pore sizes and how electrochemistry occurs on a nonconductive polymer surface. Here, we investigated the electrodeposition process step-by-step and found that the electrodeposition in the 3D polymer templates took place in two stages. At the early stage of electrodeposition (<60 min), a thin titania seed layer (~55 nm) was conformally coated on the polymer surface. Once the metal oxide surface was established, the deposition proceeded from the template bottom layer toward the top at a rate of ~0.4 $\mu$m/min. After preannealing the composite film at a lower temperature, 375 °C, followed by a low heating rate to 500 °C to remove the polymer template, we obtained a dense, anatase 3D titania crystal without pattern collapse. Scanning electron microscopy (SEM) images suggested a nearly completely filled 3D titania crystal without pinch-off of the pore network, which was further confirmed by reflectivity measurement of the films in the [111] direction at various processing stages in comparison to the calculated values.

## Experimental Section

**Fabrication of the Diamond-like Polymer Templates.** The 3D polymer template was fabricated by exposing the negative-tone photoresist, SU8, to four umbrella-like visible laser beams split from one coherent laser source ($\lambda$ = 532 nm, diode-pumped Nd:$YVO_4$ laser) following the procedure reported previously.[14] Briefly, the central beam was circularly polarized with normal incidence to the photoresist film, while the other three surrounding beams were linearly polarized and oblique at 39° relative to the central one. The wave vectors of four beams are $\mathbf{k}_0 = \pi/a[333]$, $\mathbf{k}_1 = \pi/a[511]$, $\mathbf{k}_2 = \pi/a[151]$, and $\mathbf{k}_3 = \pi/a[155]$, respectively, where $a$ is the lattice constant. The polarization vectors of beams 1, 2, and 3 are $\mathbf{e}_1$ = [−0.250 0.345 0.905], $\mathbf{e}_2$ =[−0.905 −0.250 0.345], and $\mathbf{e}_3$ =[0.345 0.905 −0.250], respectively. The circular polarization of the central beam distributes the intensity equally to the surrounding beams, at a ratio of 1.8:1:1:1.

The photoresist solution (~58 wt %) was formulated by mixing Epon SU-8 pellets and 2.0 wt % Irgacure 261 (from Ciba Specialty Chemicals) as visible photoinitiators in $\gamma$-butyrolactone (GBL, Aldrich), and spin-coated on an ITO glass at 2000 rpm for 30 s. To ensure good adhesion between the SU8 film and ITO, the latter was cleaned by ultrasonication in isopropanol and acetone, respectively, followed by oxygen plasma. The photoresist film was preexposure bake at 65 °C for 3 min and 95 °C for 40 min, resulting in film thickness of ~ 6 $\mu$m. The film was exposed to the superimposed interference beams (laser output of 1 W) for 1−2 s.

(18) Hetherington, N. B. J.; Kulak, A. N.; Sheard, K.; Meldrum, F. C. *Langmuir* **2006**, *22*, 1955.
(19) Yue, W. B.; Kulak, A. N.; Meldrum, F. C. *J. Mater. Chem.* **2006**, *16*, 408.
(20) Martin-Moreno, L.; Garcia-Vidal, F. J.; Somoza, A. M. *Phys. Rev. Lett.* **1999**, *83*, 73.
(21) Babin, V.; Garstecki, P.; Holyst, R. *Phys. Rev. B* **2002**, 66.
(22) Moon, J. H.; Xu, Y.; Dan, Y.; Yang, S. M.; Johnson, A. T.; Yang, S. *Adv. Mater.* **2007**, *19*, 1510.
(23) Moon, J. H.; Yang, S.; Yang, S. M. *Appl. Phys. Lett.* **2006**, 88.
(24) Yue, W. B.; Park, R. J.; Kulak, A. N.; Meldrum, F. C. *J. Cryst. Growth* **2006**, *294*, 69.
(25) Park, R. J.; Meldrum, F. C. *Adv. Mater.* **2002**, *14*, 1167.
(26) Lai, M.; Kulak, A. N.; Law, D.; Zhang, Z. B.; Meldrum, F. C.; Riley, D. J. *Chem. Commun.* **2007**, 3547.
(27) Andricacos, P. C.; Uzoh, C.; Dukovic, J. O.; Horkans, J.; Deligianni, H. *IBM J. Res. Dev.* **1998**, *42*, 567.
(28) Miao, Z.; Xu, D. S.; Ouyang, J. H.; Guo, G. L.; Zhao, X. S.; Tang, Y. Q. *Nano Lett.* **2002**, *2*, 717.
(29) Braun, P. V.; Wiltzius, P. *Nature* **1999**, *402*, 603.
(30) Yan, H.; Yang, Y.; Fu, Z.; Yang, B.; Xia, L.; Fu, S.; Li, F. *Electrochem. Commun.* **2005**, *7*, 1117.
(31) Lee, Y. C.; Kuo, T. J.; Hsu, C. J.; Su, Y. W.; Chen, C. C. *Langmuir* **2002**, *18*, 9942.
(32) Klein, J. D.; Herrick, R. D.; Palmer, D.; Sailor, M. J.; Brumlik, C. J.; Martin, C. R. *Chem. Mater.* **1993**, *5*, 902.
(33) Edamura, T.; Muto, J. *Thin Solid Films* **1993**, *235*, 198.

**Scheme 1. Schematic Illustration of the Electrodeposition Setup Using a Three-Electrode Cell**

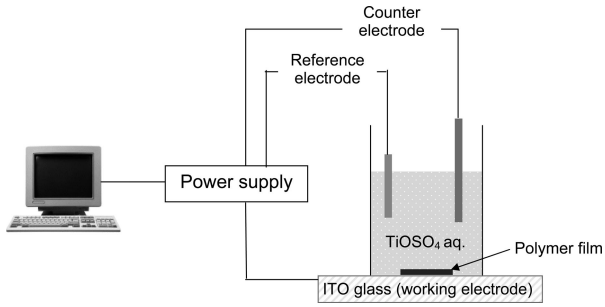


After postexposure bake (PEB) at 65 °C for 2−4 min and 95 °C for 2−4 min, respectively, the film was developed in propylene glycol monomethyl ether acetate (PGMEA, Aldrich) to remove unexposed or weakly exposed films, resulting in 3D microporous structures. To prevent the pattern collapse of the 3D film due to the capillary force by air drying, we dried the film using supercritical $CO_2$ dryer (SAMDRI-PVT-3D, tousimis) after the development.[34]

**Fabrication of 3D Titania Photonic Crystals through Electrodeposition.** The titania stock solution was prepared according to the procedure described in the literature.[28] First, the crystalline titanium powder with high purity (99.999%, Aldrich) was dissolved and oxidized in a mixture solution containing 30 vol % $H_2O_2$ and 30 vol % ammonia. The excess $H_2O_2$ and ammonia was decomposed by heating the solution to 80 °C, resulting in a yellow gel. The yellow gel was then dissolved in a 4 M aqueous $H_2SO_4$ to form a red-colored stock solution for electrodeposition. Before the deposition, ~145 mM potassium nitrate ($KNO_3$) was added in the red stock solution, and the pH of the solution was adjusted to 2−3 using the 30 vol % ammonia solution.

The electrodeposition was conducted at room temperature using a homemade three-electrode cell (Scheme 1).[35] The deposition process was monitored using an Ag/AgCl reference electrode (Bioanalytical System Inc.) with a potential range from 1.0 to 1.3 V. A Pt wire was used as the counter electrode (anode) and ITO glass as the working electrode (cathode). The current was computer controlled and maintained constant as 10 mA. The deposition rate was estimated based on SEM images at different time intervals. Because the SU8 film was relatively hydrophobic (water contact angle ~ 80 °), we first wetted the 3D polymer template with the low surface energy solvent, methanol, before immersing the template into the titania solution. After deposition, the sample was removed from the solution and rinsed with DI water. The composite film was then calcined at 500 °C in air for ~3 h at different heating conditions to obtain the inverse titania structures.

**Characterization.** The film thickness was measured by profilometer (Tencor Instruments, Alpha Step 10). The high resolution SEM images were taken from a FEI Strata DB235 focused ion beam (FIB) system at 5 kV. The powder X-ray diffraction (XRD) was performed on Rigaku Geigerflex diffractometer using Cu as the target, and the $2\theta$ angle was varied from 16° to 80° with a counting rate of 0.5 counts/min. The reflectivity spectra were acquired using Varian Excalibur FTS-3000 equipped with a 600 UMA microscope and Varian FTS-7000 with a 600 UMA microscope, respectively. The samples were measured with the aperture size of ~100 $\mu$m × 100 $\mu$m. The photonic bandgap properties of the crystal structures obtained at different processing steps were calculated by the MIT Photonic-Band Package, where the refractive indices of 1.6, 2.2,[17] and 2.5[36] were used for SU8, amorphous titania, and anatase titania, respectively.

## Results and Discussions

Both experimental studies[14,16] and calculation[22] have suggested that it is nearly impossible to completely fill the holographically patterned, triply periodic bicontinuous templates through a top-down, conformal coating process due to the pinch-off problem. Electrodeposition, however, has shown promise to nearly completely fill a three-term diamond-like polymer template with titania sol−gel.[22] Questions remain about how the electrodeposition occurs and evolves within the insulating 3D polymer template because the electrodeposited materials often grow from the (semi-)conductive substrate and what the actual filling fraction of titania is within the template. In addition of SEM images, more quantitative characterization and analysis, such as reflectance measurement of the obtained 3D photonic crystals, will be necessary to reveal the nature of backfilling and the photonic bandgap properties of the film.

Our electrodeposition procedure was modified from the one demonstrated by Miao et al.,[28] which grows $TiO_2$ nanowires from an AAO membrane on a Au substrate. The AAO and Au substrate act as the working electrodes. First, the nitrate ions are electro-reduced to generate hydroxide ions, which increase the local pH and hydrolyze the Ti precursor to form a dispersion of sol particles on the charged surface:

$$NO_3 + 6H_2O + 8e^- \rightarrow NH_3 + 9OH^- \quad (1)$$

$$TiO^{2+} + 2OH^- \rightarrow TiO(OH)_2(sol) \quad (2)$$

As the electrochemistry proceeds, the sol particles are cross-linked to form the titanium oxyhydroxide gel network.

$$TiO(OH)_2(sol) - xH_2O \rightarrow TiO_{1+x}(OH)_{2-2x}(gel) \quad (3)$$

In comparison to the conventional sol−gel backfilling, this approach offers several advantages that appear attractive to completely fill the triply periodic bicontinuous structures. First, the electrochemistry generates high local pH and a pH gradient within the pore channel, leading to formation of a compact film from the template bottom up and filling small pores (diameter ≤ 20 nm). Second, the deposition thickness can be controlled by varying the deposition time and current or potential of the counter electrode. Third, the deposition rate could be manipulated by the concentration of $KNO_3$ solution and/or the current or potential of the counter electrode.

**Fabrication of 3D Polymer Templates.** The polymer template was fabricated on a conductive, transparent ITO glass substrate using four-beam interference lithography of the SU8 film. ITO acts as the working electrode while the transparency is important for holographic lithography, which requires minimal reflection from the substrate. To facilitate the deposition of the titania sol within (sub)-micrometer pores

(34) Yang, S.; Megens, M.; Aizenberg, J.; Wiltzius, P.; Chaikin, P. M.; Russel, W. B. *Chem. Mater.* **2002**, *14*, 2831.
(35) Natarajan, C.; Nogami, G. *J. Electrochem. Soc.* **1996**, *143*, 1547.
(36) Rocquefelte, X.; Goubin, F.; Koo, H. J.; Whangbo, M. H.; Jobic, S. *Inorg. Chem.* **2004**, *43*, 2246.

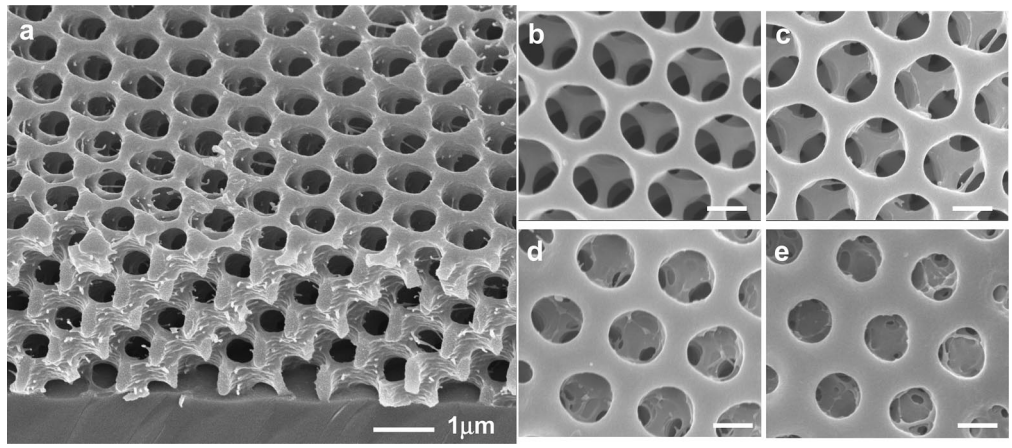


**Figure 1.** SEM images of SU8 diamond-like structures fabricated by holographic lithography with postexposure baking (PEB) at 95 °C. (a) Cross-sectional view with 2.0 min PEB time. (b−e) Top views at different PEB times: (b) 2.0 min, (c) 2.2 min, (d) 2.5 min, and (e) 2.7 min. Scale bars: 500 nm.

while maintaining the film integrity during the electrochemical reaction, it is important to optimize the filling fraction of the porous film. As shown earlier,[34] the film porosity can be varied from 10 to 80% by changing the exposure time and intensity. Here, we first optimized the exposure time and intensity to obtain a robust film with porosity in the range of 40−60%. We then varied the PEB time to fine-tune the filling fraction. As shown in Figure 1, for fixed exposure time (1−2 s) and intensity (laser output of 1 W), larger porosity was obtained when PEB was at 95 °C for a shorter period. The film that was PEB for 2.0 min (Figure 1a,b) was chosen for the subsequent study of electrodeposition. The characterization of the filling fraction will be discussed later.

**Mechanistic Study of Electrodeposition within the 3D Polymer Templates.** It is known that the hydrolysis and gelation of sol−gels is strongly dependent on the solution pH. In our experiments, we maintained the current relatively low, 10 mA, and the concentration of $KNO_3 \leq 145$ mM. At a higher $KNO_3$ concentration (e.g., 290 mM), a large amount of ammonia was quickly generated, resulting in immediate formation of yellow titania gel that was broken into small pieces and floated toward the air−water interface. No deposition within the porous template was observed.

To understand the electrodeposition mechanism within the 3D polymer template, we examined the polymer/titania composite structures by SEM at different deposition time intervals. At the early deposition stage (deposition time < 60 min), a thin titania layer appeared to be conformally coated on the SU8 template (Figure 2). In comparison to the polymer template (Figure 1a), the titania coated pore surface appeared rough and more rounded with a decreased pore size. The thickness of the titania layer was estimated to be ∼55 nm at a deposition time of ∼58 min from the SEM image (Figure 2a vs Figure 1a). The cross-sectional view (Figure 2c) further revealed that there was no infiltration of the titania into the bottom layers at this stage. It has been suggested that in electroplating of interconnects in integrated circuits,[27] to coat metal or alloy over the entire surface of a patterned, insulating structure, it is first necessary to conformally deposit a seed layer, which conducts current from the electrode to the surface where a deposit is desired. Because SU8 is nonconductive, we believe that building up

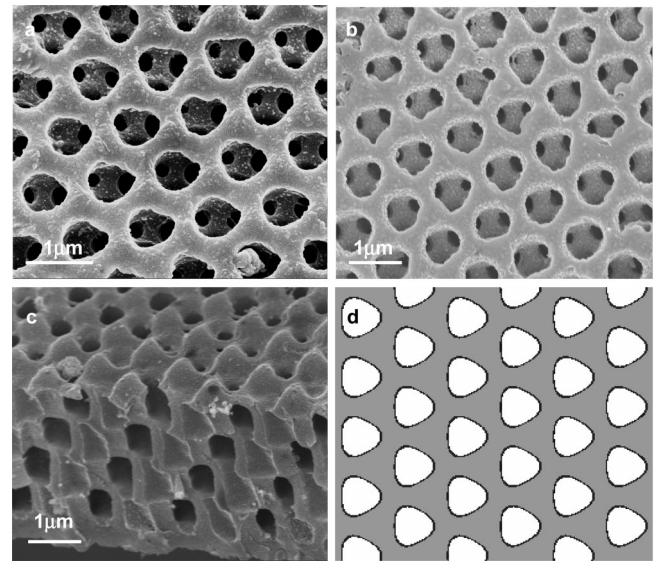


**Figure 2.** (a−c) SEM images of the conformal coating of $TiO_2$ on the SU8 template at the early deposition stage (deposition time of ∼58 min). (a) Film top layer, (b) film bottom layer, and (c) cross-sectional view. (d) Simulated 2D view of the conformal coating in the (111) plane of the template.

a thin conformal coating of $TiO_2$ as "seed" layer on the polymer template at the initial stage is a critical step toward the subsequent electrodeposition throughout the 3D microporous template. Figure 2d is the schematic 2D view of the conformal coating on the template surface in the (111) plane.

Once the seed layer was established, the deposition proceeded rather quickly. The 3D SU8 template (∼6 $\mu$m thick) was nearly completely filled within 15 min (Figure 3) at a rate of ∼ .4 $\mu$m/min in a bottom-up fashion. Figure 3 shows the SEM images of a free-standing $TiO_2$/SU8 composite film upside down. At the deposition time of ∼60 min, the first bottom layer began to be partially infiltrated (Figure 3a). At ∼65 min, the second bottom layer was filled (Figure 3b), and the infiltration was completed at ∼75 min (Figure 3c). Because the bottom ITO substrate is more conductive than the sides of the template coated with titania, it is expected that the local current density and, therefore, the concentration of $OH^-$ groups should be much higher at the template bottom layer than that on the sidewalls (Figure

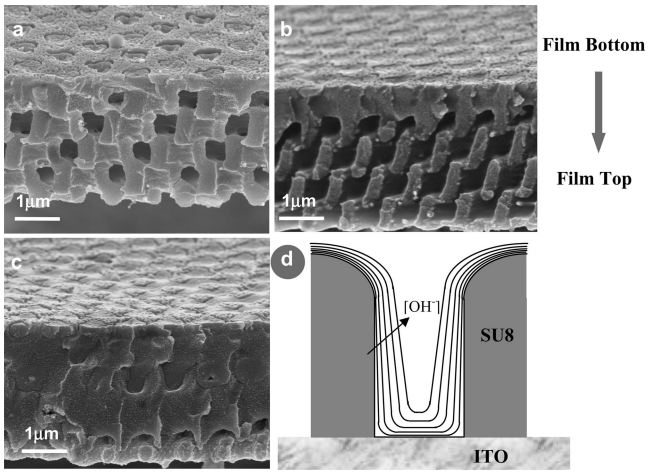


**Figure 3.** (a−c) Cross-sectional SEM images of SU8/$TiO_2$ composite shown upside down at different deposition time intervals: (a) ∼60 min, (b) ∼65min, and (c) ∼75 min, respectively. (d) Schematic illustration of $OH^-$ concentration contour lines with a pH gradient between the bottom and sidewall in a porous channel (not to scale).

3d). The high local pH at the bottom layer leads to more complete hydrolysis and condensation, resulting in formation of a relatively compact film and, therefore, further restricts the transport of ions to the upper layer.[28] As the deposition proceeds, the pH gradient increases with decrease of the pore size, causing a much higher deposition rate at the second deposition stage. The cross-sectional SEM image of the composite (Figure 3c) shows no obvious pinch-off of pore network in comparison to that seen in silica/SU8 structures filled by the CVD process.[14,22] For void-free filling, a higher deposition rate at the template bottom than on the sidewalls is desired,[27] which can be attributed to the diffusion-controlled $OH^-$ concentration and the pH gradient. Similar strategy has been applied in damascene Cu plating[27] to seamlessly deposit Cu defect-free within lithographically patterned cavities, which have vertical walls and high aspect ratios, by using additives to inhibit the transport of cupric ion, $Cu^{2+}$. The deposition rate is much higher at the bottom of the feature where the diffusion-controlled inhibitor concentration is the lowest.

**Calcination of the Composite Films and Film Shrinkage.** After the backfilling, the polymer/titania composite was calcined at 500 °C to remove the polymer template, resulting in the inverse titania photonic crystal. It is important though to preanneal the sample and optimize the heating rate to densify the titania gel before removal the polymer template to prevent film collapse.[37] Here, we purposely used the titania/SU8 composite with thin titania conformal coating (∼55 nm, Figure 2a) to optimize the calcination conditions. As seen in Figure 4a, when the composite was directly heated to 500 °C at a fast heating rate of 9 °C/min in air, the titania skeleton was not condensed enough to withstand the high calcination temperature, resulting in a rather porous and nearly collapsed film. In contrast, when the composite was preannealed at 375 °C for ∼7 h in air, followed by a slow ramping rate (3 °C/min) to 500 °C, a rather robust and dense titania skeleton was observed (Figure

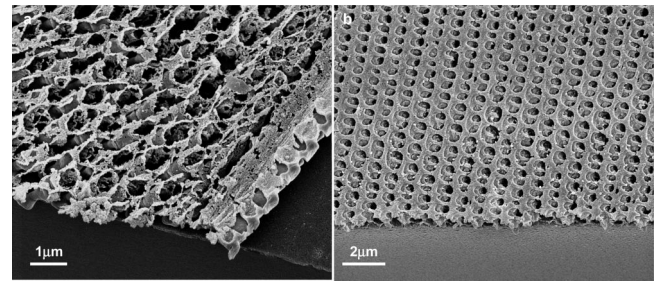


**Figure 4.** SEM images of inverse titania 3D skeletons obtained from electrodeposition for ∼58 min on the SU8 template, followed by different calcination conditions: (a) direct ramping to 500 °C in air at a rate of 9 °C/min without preannealing and (b) preannealing at 375 °C for ∼7 h in air, followed by heating to 500 °C at a rate of 3 °C/min and held at 500 °C for 3 h.

4b). It has the same 3D structure as the original polymer template (Figure 1a), which further confirms the conformal coating of titania on polymer template at the early electrodeposition stage. For the 3D titania film that was electrodeposited for ∼79 min, followed by the two-step calcination process, we can clearly see a very dense titania film without any unfilled pore voids or nanopores (Figure 5).

During preannealing and calcination steps, the sol−gel film is further densified, thus, large film shrinkage is often expected.[38,39] Cracks will occur and propagate if the film is attached to the substrate due to the residue strain generated from the shrinkage and the mismatch of the coefficient of thermal expansion between the titania and the substrate. To quantify the shrinkage of the 3D titania film fabricated by the electrodeposition technique, which would be important to the later photonic bandgap simulation, we compared the periodicity of titiania crystal with that of the SU8 template in the (111) plane and [111] direction (see Table 1). The shrinkage in the (111) plane is 26.8%, whereas that in the [111] direction is 33.3% with the film attached to the substrate (Table 1). Typically there are areas of a few hundreds of micrometers wide crack-free and suitable for the optical characterization. When the film is lifted-off from the substrate before calcination, allowing for more uniform shrinkage, a titania film with far fewer cracks can be obtained.

**Crystallinity of the Calcined Titania.** Titania could have several crystalline phases with different refractive indices, including anatase, rutile, and their mixtures. When the $TiO_2$ gel is sintered at 500 °C, the anatase phase[40] is often obtained with a refractive index of 2.5,[41] which can be completely converted to rutile ($n$ ∼2.70−3.0) at 1000 °C. Using the powder X-ray diffraction (XRD) technique, we characterized the bulk titania film deposited on the ITO glass outside of the patterned region, which was calcined at 500 °C for 3 h. Figure 6 shows peaks at $2\theta$ = 25.4°, 38.3°, 48.1°, 55.2°, and 62.3°, corresponding to the different crystal planes in

(37) Chabanov, A. A.; Jun, Y.; Norris, D. J. *Appl. Phys. Lett.* **2004**, *84*, 3573.
(38) Campbell, M.; Sharp, D. N.; Harrison, M. T.; Denning, R. G.; Turberfield, A. J. *Nature* **2000**, *404*, 53.
(39) Wijnhoven, J.; Vos, W. L. *Science* **1998**, *281*, 802.
(40) Wang, C. C.; Ying, J. Y. *Chem. Mater.* **1999**, *11*, 3113.
(41) Gu, Z. Z.; Kubo, S.; Qian, W. P.; Einaga, Y.; Tryk, D. A.; Fujishima, A.; Sato, O. *Langmuir* **2001**, *17*, 6751.

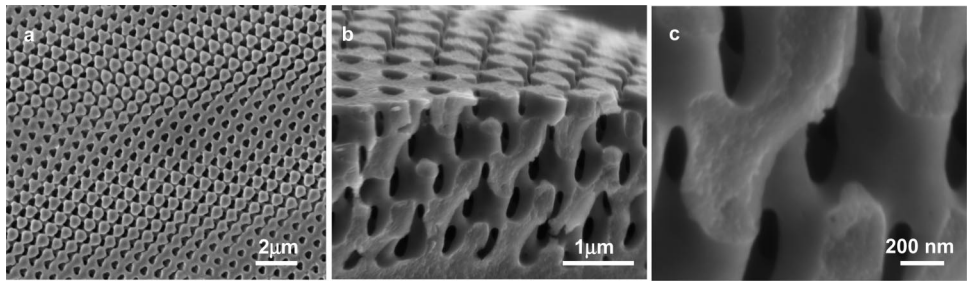


**Figure 5.** SEM images of the inverse 3D titania crystals after preannealing at 375 °C and calcination at 500 °C for 3 h. (a) Top view and (b, c) cross-sectional views at different magnifications. The film was electrodeposited for ~79 min.

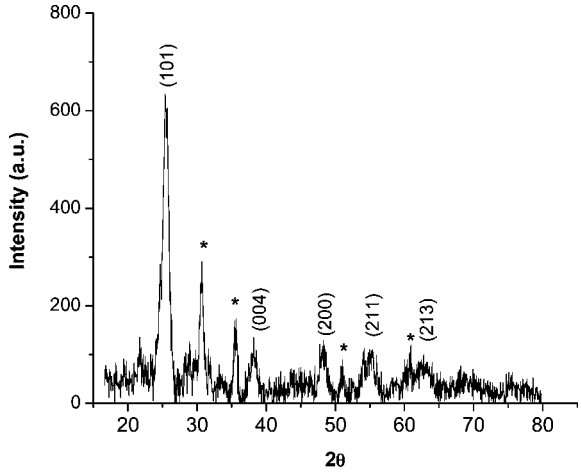


**Figure 6.** XRD diffraction pattern of the bulk titania film after calcination at 500 °C for 3 h. (*) Peaks from the ITO glass substrate.

**Table 1. Comparison of Periodicity in the Inverse 3D Titania Crystal with That in the SU8 Template**[a]

| periodicity | SU8 template | titania crystal | film shrinkage |
|---|---|---|---|
| in the (111) plane ($\mu$m) | 0.97 | 0.71 | 26.8% |
| in the [111] direction ($\mu$m) | 2.43 | 1.62 | 33.3% |

[a] The titania film was preannealed at 375 °C for ~7 h in air, followed by heating to 500 °C at a rate of 3 °C/min, and held at 500 °C for 3 h. The SU8 films were milled by focus ion beam (FIB) perpendicularly to the (111) plane with an output current of 1000 pA.

the anatase titania, whereas those at $2\theta = 30.7°$, 35.6°, 51.0°, and 60.9° are assigned to the ITO glass substrate.[42]

**Optical Characterization of the 3D Photonic Crystals.** To quantitatively evaluate the completeness of the backfilling, we measured the reflectance of the photonic crystals (SU8, SU8/$TiO_2$ composite, and inverse $TiO_2$) obtained at different processing steps in the [111] direction and compared them with the calculated PBG (Figure 7). The PBG was calculated by considering the structure distortion due to the refractive effect at the air−film interface and film shrinkage after lithography and calcination steps.[43]

In the reflectance spectrum of the SU8 template (Figure 7a), the interference fringes are related to film thickness $t$ as[44]

$$t = \frac{\Delta m}{2n_{\text{eff}}(v_1 - v_2)} \quad (4)$$

where $n_{\text{eff}}$ is the effective refractive index, $\Delta m$ is the number of fringes, and $v_1$ and $v_2$ are the wavenumbers of different fringes. For $t = 6.0$ $\mu$m, we obtain the effective refractive index of the film, $n_{\text{SU8/air}} = 1.3$. The filling volume fraction can be estimated by[41]

$$n_{\text{eff}}^2 = f_1 n_1^2 + (1 - f_1) n_2^2 \quad (5)$$

where $n_1$ and $n_2$ are the refractive indices of components 1 and 2, respectively, and $f_1$ is the filling volume fraction of component 1. For $n_{\text{SU8}} = 1.6$ and $n_{\text{air}} = 1$, we obtain $f_{\text{SU8}} = 44\%$, which is the same as that estimated from the reconstructed 3D SU8 structure using SEM images from different cleavage planes. There was a 10% red shift (0.1−0.2 $\mu$m) of the experimentally observed peak position at $\lambda = 2.4$ $\mu$m with respect to the calculated PBG in the [111] direction between the second and third bands (Figure 7a). We measured the reflectance spectrum of the 3D SU8 film from three different research groups using both Varian Excalibur FTS-3000 and Varian FTS-7000 and confirmed that the reflectance peak always appeared at 2.4 $\mu$m. We think the small discrepancy in peak location between experiment and calculation may be due to the experimental error, which could slightly shift the level surface of the fabricated 3D structure, or simply be due to the nonuniform porosity caused by the Gaussian distribution of the laser intensity.[14]

Compared to the SU8 template, there was a bathochromic shift of the reflection peak to ~3.2 $\mu$m in the SU8/$TiO_2$ composite (Figure 7b) as a result of the increase of the mean dielectric field of the composite even though there is a decrease of the refractive index contrast. According to Bragg's Law, at the normal incidence to the (111) plane the reflectance peak wavelength is

$$\lambda = 2d_{111}n_{\text{eff}} \quad (6)$$

where $d_{111}$ is the interlayer distance in the [111] direction. For $d_{111} = 0.81$ $\mu$m (measured from SEM), we estimate that the effective refractive index for the composite is $n_{\text{SU8/TiO}_2} \approx 2.0$, which agrees with the reported value in the literature.[45] Therefore, the refractive index of the as-deposited titania film is estimated by eq 5 as $n_{\text{TiO}_2\text{/as-deposited}} = 2.2$, corresponding to that of amorphous titania.[17] Figure

(42) Sasagawa, M.; Nosaka, Y. *Phys. Chem. Chem. Phys.* **2001**, *3*, 3371.
(43) Zhu, X.; Xu, Y.; Yang, S. *Opt. Express* **2007**, *15*, 16546.
(44) Wong, D.; Tan, T. L.; Lee, P.; Rawat, R. S.; Patran, A. *Microelectron. Eng.* **2006**, *83*, 1912.
(45) Schroden, R. C.; Al-Daous, M.; Blanford, C. F.; Stein, A. *Chem. Mater.* **2002**, *14*, 3305.

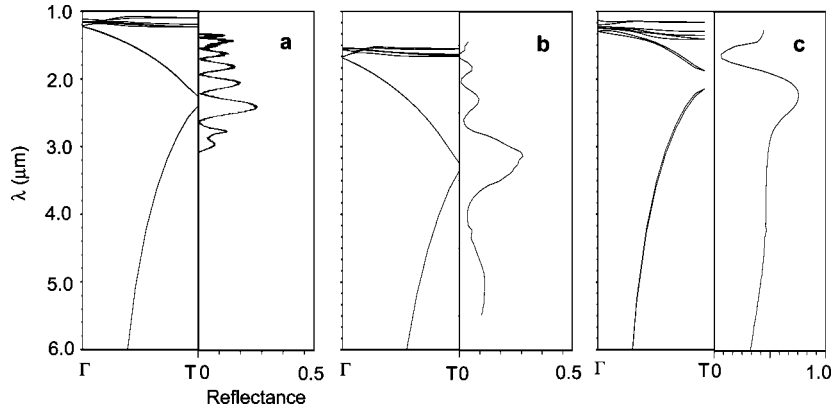


**Figure 7.** FTIR reflectance spectra of 3D diamond-like structures in the [111] direction: (a) SU8, (b) SU8/$TiO_2$, and (c) inverse $TiO_2$. In each panel, the left figure is a simulated spectrum, and the right one is the experimental data.

**Table 2. Comparison of the Optical Properties and Filling Volume Fractions of the 3D Photonic Crystals Obtained at Different Processing Steps**

| | | | filling volume fraction | |
|---|---|---|---|---|
| photonic crystals | reflectance peak position ($\mu$m) | effective refractive index of film ($n_{eff}$) | component 1 | component 2 |
| SU8/air | 2.4 | 1.3 | $f_{SU8} = 44\%$ | $f_{air} = 56\%$ |
| SU8/$TiO_2$ | 3.2 | 2.0 | $f_{SU8} = 44\%$ | $f_{TiO_2} = 56\%$ |
| air/$TiO_2$ | 2.2 | 2.0 | $f_{air} = 43\%$ | $f_{TiO_2} = 57\%$ |

7b clearly shows that the reflection peak of the SU8/$TiO_2$ structure matches well with the calculated peak position. More strikingly, the estimated volume fraction of the amorphous $TiO_2$, 56%, is exactly the same as the air volume fraction in the SU8 template, which undoubtedly confirms that the SU8 template is nearly completely filled by the electrodeposition method.

After calcination to remove the polymer template, the reflection peak of the 3D inverse $TiO_2$ crystal blue-shifted to ~2.2 $\mu$m, which agrees reasonably well with the calculated peak position assuming $f_{TiO_2/anatase} = 56\%$ (Figure 7c). The reflectance peak appeared rather broad though, which might be attributed to the finite size of the sample (~200 $\mu$m) in the FTIR measurement. The peak reflectivity increased from 24% for SU8 to 76% for inverse $TiO_2$ (anatase) photonic crystals, indicating increased optical quality of the film. From Bragg's Law, the effective index for the inverse $TiO_2$ structure is calculated as $n_{TiO_2/air} = 2.0$. Assuming $n_{TiO_2/anatase} = 2.5$,[36] we obtain the filling volume fraction of titania, $f_{TiO_2/anatase} = 57\%$. It again agrees well with volume fraction of the air in the SU8 template, $f_{air} = 56\%$ (Table 2), further supporting the complete filling of titania sol−gel into the polymer template through the electrodeposition process. It is noted that the lattice constant of the calcined titania crystal is smaller than that of the polymer template. Therefore, the similarity between the titania filling volume fraction in the inverse titania crystal and the air volume fraction in the polymer template suggests that the 3D structure is well-preserved during the backfilling and calcination steps.

## Conclusion

We systematically studied the backfilling of the holographically patterned diamond-like polymer templates with titania sol−gel using the electrodeposition technique. The electrodeposition appeared to proceed in two stages (Scheme 2). At the early stage of electrodeposition (<60 min), a thin titania film was conformally coated on the surface of polymer template, creating a seed layer that appeared critical for further bottom up electrodeposition. In the second stage, the deposition rate on the existing titania surface increased significantly at a rate of 0.4 $\mu$m/min, and the deposition occurred preferentially from the film bottom layer, which could be attributed to the diffusion-controlled hydroxyl ion concentration and a pH gradient within the template. SEM images suggested there was no pinch-off of the pore network after the backfilling. After calcination at 500 °C to remove the polymer template, a nearly completely filled inverse 3D titania structure was obtained. We showed that a combination of preannealing step and a slow heating rate was important to form a dense 3D anatase titania crystal without pattern collapse. The optical properties of the 3D photonic crystals were measured at various processing steps and compared with the PBG calculation. The nearly perfect agreement

**Scheme 2. Schematic Illustration of the Electrodeposition Process to Backfill Titania Sol−Gel into the 3D SU8 Template**

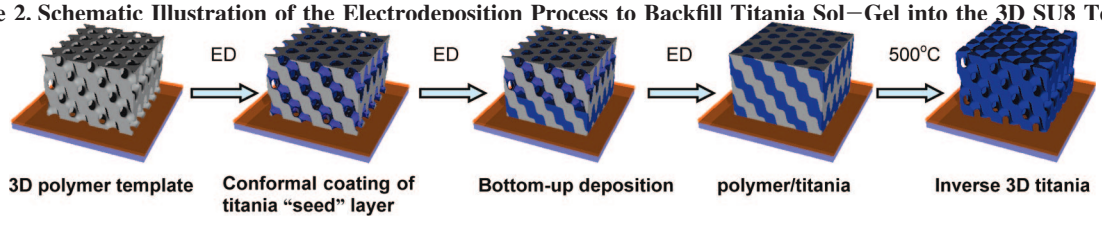

of the experimental reflectance spectra with the simulated ones, and thus the obtained volume fraction at each step, strongly supported the SEM observation: that is, the polymer template was nearly completely filled with titania by the bottom-up process. Although the study reported here focuses on electrodeposition of titania sol−gel, we believe the understanding of the backfilling mechanism will offer important insights to broaden the application of templating approaches and deposition of other high index materials.

**Acknowledgment.** We thank Robert Norwood (University of Arizona) for providing the FTIR reflectance measurement data of SU8 3D structures for comparison to confirm the reflectance peak location and his insightful discussion. We acknowledge Drexel Materials Characterization Facility for FTIR measurements. This research is supported by the Office of Naval Research (ONR), Grant N00014-05-0303, and NSF NIRT (Grant ECS-0303981).

CM702511K